

Biochemical clocks and molecular noise: Theoretical study of robustness factors

D. Gonze and J. Halloy

Unité de Chronobiologie Théorique, Faculté des Sciences, Université Libre de Bruxelles, Campus Plaine, Code Postal 231, B-1050 Brussels, Belgium

P. Gaspard

Center for Nonlinear Phenomena and Complex Systems, Faculté des Sciences, Université Libre de Bruxelles, Campus Plaine, Code Postal 231, B-1050 Brussels, Belgium

(Received 24 December 2001; accepted 12 March 2002)

We report a study of the influence of molecular fluctuations on a limit-cycle model of circadian rhythms based on the regulatory network of a gene involved in a biochemical clock. The molecular fluctuations may become important because of the low number of molecules involved in such genetic regulatory networks at the subcellular level. The molecular fluctuations are described by a birth-and-death stochastic process ruled by the chemical master equation of Nicolis and co-workers and simulated by Gillespie's algorithm. The robustness of the oscillations is characterized, in particular, by the probability distribution of the first-return times and the autocorrelation functions of the noisy oscillations. The half-life of the autocorrelation functions is studied as a function of the size of the system which controls the magnitude of the molecular fluctuations and of the degree of cooperativity of some reaction steps of the biochemical clock. The role of the attractivity of the limit cycle is also discussed. © 2002 American Institute of Physics. [DOI: 10.1063/1.1475765]

I. INTRODUCTION

When driven far from the thermodynamic equilibrium, chemical or biochemical reactions may generate oscillations. In macroscopic systems, such reactions are described by nonlinear differential equations ruling the time evolution of the chemical concentrations according to the laws of chemical kinetics. Oscillating reactions correspond to periodic solutions of these equations. However, such a macroscopic description does not take into account the molecular fluctuations which become important in systems with a low number of molecules. The question arises as to whether the sustained oscillations predicted by the macroscopic description are robust with respect to the molecular noise caused by the low number of molecules. This question is of fundamental importance for the biochemical reactions of the intracellular regulatory processes,¹ especially for the reactions involved in gene expression.²⁻⁵ This is the case for the circadian rhythms of 24 hours which are observed not only in pluricellular organisms such as plants, insects or vertebrates, but also in unicellular organisms such as cyanobacteria (reviewed in Refs. 6, 7). Recent work has indeed revealed that circadian rhythms are controlled by biochemical clocks which can be observed at the level of single cells.^{8,9} In this context, a fundamental problem is to understand how the molecular fluctuations affect the robustness of such biochemical clocks in intracellular systems with a low number of molecules (i.e., proteins, mRNAs, ...).¹⁰⁻¹² The purpose of the present paper is to present a theoretical study of the robustness factors in a recently proposed model of circadian rhythms.

In living organisms, a common origin of the circadian clocks rests on a genetic control: a clock protein exerts a

repression on the transcription of its own gene.^{6,7} Models for biological clocks based on this negative regulation have been proposed for the PER protein in the fly *Drosophila*^{13,14} and for the FRQ protein in the fungus *Neurospora*.¹⁵ However, several other genes involved in this mechanism have been identified such as, in *Drosophila*, the *tim* gene responsible for the TIM protein which forms a complex with the PER protein able to enter into the nucleus.¹⁶ An extended model incorporating TIM has been studied.¹⁷ Furthermore, the genes *clk* and *cyc* are required for the activation of the *per* and *tim* transcription. The effect of the PER-TIM protein complex is to repress the *per* and *tim* transcription by inhibiting the CLK-CYC complex activity.^{18,19} A second feedback loop is achieved by the *clk* activation caused by the PER-TIM complex.¹⁸ In *Neurospora*, the proteins WC-1 and WC-2 play a similar role as CLK and CYC: they form a complex able to activate the transcription of the *frq* gene and the FRQ protein inhibits this activity.^{20,21} Updated models taking into account these additional regulations are currently investigated.^{22,23}

The core mechanism of these biological clocks can be described by a minimal model, including only three variables, initially proposed for circadian rhythms in *Neurospora*.¹⁵ Here, we focus for simplicity on this minimal model for which we present theoretical methods and numerical simulations to quantify the effect of molecular noise on the robustness of the oscillations.

The molecular fluctuations are taken into account by a birth-and-death stochastic process describing the random time evolution of the biochemical clock. This stochastic process is defined by the chemical master equation of Nicolis and co-workers²⁴⁻²⁶ and it can be simulated by Gillespie's

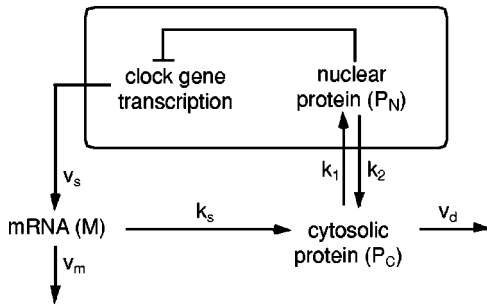


FIG. 1. Model for the molecular mechanism of circadian rhythms. The model incorporates the transcription of the gene involved in the biochemical clock and the transport of mRNA (M) into the cytosol where it is translated into the related clock protein (P_C) and degraded. The protein can be degraded or transported into the nucleus (P_N) where it exerts a negative feedback of cooperative nature on the expression of its gene.

algorithm.^{27,28} In the weak-noise limit, the chemical master equation reduces to a generalized Fokker-Planck equation which can be analyzed with a Hamilton-Jacobi method. This method allows us to obtain a theoretical expression for the probability distribution of the fluctuations of the periods, as well as for the correlation time between successive oscillations.²⁹ This correlation time characterizes the robustness of the biochemical clock under the effect of the molecular noise. This correlation time (or half-life) is then calculated for the aforementioned model of circadian rhythms. In this way, several factors of robustness are identified and discussed.

The paper is organized as follows. The model is presented in Sec. II. The stochastic simulations are described in Sec. III. The theory is developed in Sec. IV. The results are presented and discussed in Sec. V. Conclusions and perspectives are drawn in Sec. VI.

II. PRESENTATION OF THE MODEL

The core mechanism of circadian rhythmicity relies on the negative regulation exerted by a clock protein (i.e., FRQ in *Neurospora*, PER in *Drosophila*) on the transcription of its gene (*frq* or *per*) into the messenger RNA (mRNA), the translation of which leads to the synthesis of the clock protein. The time evolution of the three variables involved in the minimal model (Fig. 1) is governed by the following kinetic equations:¹⁵

$$\begin{aligned} \frac{d[M]}{dt} &= v_s \frac{k_I^n}{k_I^n + [P_N]^n} - v_m \frac{[M]}{k_m + [M]}, \\ \frac{d[P_C]}{dt} &= k_s [M] - v_d \frac{[P_C]}{k_d + [P_C]} - k_1 [P_C] + k_2 [P_N], \\ \frac{d[P_N]}{dt} &= k_1 [P_C] - k_2 [P_N]. \end{aligned} \quad (1)$$

In these equations, the three variables $[M]$, $[P_C]$, and $[P_N]$ denote, respectively, the concentrations (defined with respect to the total cell volume) of the clock gene mRNA and of the cytosolic and nuclear forms of the clock protein. The parameter v_s denotes the rate of transcription, k_I is the threshold beyond which the nuclear protein represses the

transcription of its gene. This repression is characterized by the Hill coefficient n . This coefficient is determined by the degree of cooperativity of this reaction, i.e., the number n of molecules which have to bind together to promote the reaction. The other parameters are the maximum rate v_m of mRNA degradation and the Michaelis constant k_m related to the latter process, the apparent first-order rate constant k_s measuring the rate of protein synthesis which is assumed to be proportional to the amount of mRNA present in the cytosol, the maximum rate v_d of protein degradation, and the Michaelis constant k_d related to this process, and the apparent first-order rate constants k_1 and k_2 characterizing the transport of the protein into and out of the nucleus.

This model as well as extended models account for circadian sustained oscillations of clock gene mRNA and clock protein in continuous darkness and has been used to study several properties of circadian rhythms such a entrainment by light-dark cycle and phase resetting following a light pulse.^{15,17,30} In an extended model taking into account more detailed mechanism of enzymatic kinetics^{11,12} similar results have been obtained as for the minimal model (1) presented here.

III. STOCHASTIC SIMULATIONS

The stochastic simulations have been carried out by means of the Gillespie algorithm.^{27,28} This method simulates the master equation in a relatively simple manner for set of reactions $\rho = 1, 2, \dots, r$ of the form

$$\sum_{i=1}^s \nu_{<\rho}^i X^i \rightarrow \sum_{i=1}^s \nu_{>\rho}^i X^i \quad (2)$$

of stoichiometric coefficients $\nu_{\rho}^i = \nu_{>\rho}^i - \nu_{<\rho}^i$ and transition rates $W_{\rho}(\{X^i\})$ (s being the number of species).

Initially, the numbers of molecules X^i of the different species $i = 1, 2, \dots, s$ are specified and the transition rates W_{ρ} of the reactions $\rho = 1, 2, \dots, r$ are computed (here, $s = 3$ and $r = 6$). A cumulative function is built by

$$c_{\rho} = \sum_{\rho'=1}^{\rho} \frac{W_{\rho'}}{c_0} \quad \text{with} \quad c_0 = \sum_{\rho=1}^r W_{\rho}. \quad (3)$$

TABLE I. Transition rates of the different reaction steps entering the chemical master equation (6). We notice that the transition rates are proportional to the extensivity parameter Ω . These transition rates imply the macroscopic equations (1), as shown in Eqs. (17) and (25).

Reaction step	Transition rate	Transitions
$G \rightarrow M + G$	$W_1 = v_s \frac{k_I^n \Omega}{k_I^n + (P_N/\Omega)^n}$	$M \rightarrow M + 1$
$M \rightarrow$	$W_2 = v_m \frac{M}{k_m + (M/\Omega)}$	$M \rightarrow M - 1$
$M \rightarrow P_C + M$	$W_3 = k_s M$	$P_C \rightarrow P_C + 1$
$P_C \rightarrow$	$W_4 = v_d \frac{P_C}{k_d + (P_C/\Omega)}$	$P_C \rightarrow P_C - 1$
$P_C \rightarrow P_N$	$W_5 = k_1 P_C$	$P_C \rightarrow P_C - 1, P_N \rightarrow P_N + 1$
$P_N \rightarrow P_C$	$W_6 = k_2 P_N$	$P_C \rightarrow P_C + 1, P_N \rightarrow P_N - 1$

Then, two random numbers, z_1 and z_2 , are generated which are uniformly distributed in the unit interval. The first one serves to determine the time interval to the next reaction step, according to

$$\Delta t = -\frac{1}{c_0} \ln(z_1) \quad (4)$$

and the second one is used to determine which reaction step occurs during this time interval: If $c_{\rho-1} < z_2 < c_\rho$, it is the reaction step ρ that takes place. The system is then updated according to

$$\begin{aligned} t &\rightarrow t + \Delta t, \\ X^i &\rightarrow X^i + \nu_\rho^i \text{ for all species } i \\ &\text{involved in the reaction } \rho \end{aligned} \quad (5)$$

and the transition rates W_ρ are recomputed given the new chemical populations and all operations are repeated until the final time t_{\max} is reached.

In the Gillespie method, an extensivity parameter Ω allows the control of the size of the system and hence the maximum number of molecules that can be present. The extensivity parameter Ω relates the numbers X^i of molecules to the concentrations $x^i = [X^i] = X^i/\Omega$.

The six reaction steps of the model for the circadian clock illustrated in Fig. 1 and described by Eqs. (1) are listed in Table I. A transition rate W_ρ ($\rho = 1, 2, \dots, 6$) is associated with each of these reaction steps.

The Gillespie algorithm generates a birth-and-death stochastic process which is described by the following chemical master equation

$$\begin{aligned} \frac{d}{dt} P(M, P_C, P_N, t) = &+ W_1(P_N)P(M-1, P_C, P_N, t) - W_1(P_N)P(M, P_C, P_N, t) + W_2(M+1)P(M+1, P_C, P_N, t) \\ &- W_2(M)P(M, P_C, P_N, t) + W_3(M)P(M, P_C-1, P_N, t) - W_3(M)P(M, P_C, P_N, t) \\ &+ W_4(P_C+1)P(M, P_C+1, P_N, t) - W_4(P_C)P(M, P_C, P_N, t) + W_5(P_C+1)P(M, P_C+1, P_N-1, t) \\ &- W_5(P_C)P(M, P_C, P_N, t) + W_6(P_N+1)P(M, P_C-1, P_N+1, t) - W_6(P_N)P(M, P_C, P_N, t). \end{aligned} \quad (6)$$

This equation gives the time evolution of the probability $P(M, P_C, P_N, t)$ to find M molecules of mRNA, P_C cytosolic clock proteins, and P_N nuclear clock proteins. Because this probability depends only on the previous state of the system, this description pertains to Markov processes.

We notice that the master equation (6) is here applied to a system composed of two intracellular compartments, i.e., the nucleus and the cytosol. Each compartment is supposed to be homogeneous and relatively well-stirred on the time scale of the reactions, which are the conditions of validity of the chemical master equation.²⁵ We implicitly assume that cellular transport processes are efficient and we take them into account in the kinetic scheme and in the parameter values.

IV. THEORY

In this section, we derive a formula for the correlation time of the noisy oscillations. We start from the chemical master equation (6) which we first reduce to a generalized Fokker-Planck equation ruling the time evolution of the chemical concentrations:

$$x^1 \equiv [M] = \frac{M}{\Omega}, \quad (7)$$

$$x^2 \equiv [P_C] = \frac{P_C}{\Omega}, \quad (8)$$

$$x^3 \equiv [P_N] = \frac{P_N}{\Omega} \quad (9)$$

of the clock mRNA, the cytosolic clock protein, and the nuclear clock protein, respectively.

Thereafter, we find a solution of the generalized Fokker-Planck equation in the weak-noise limit by using the Hamilton-Jacobi method.³¹⁻³⁴ This solution is expanded around the periodic solution of the deterministic system, called the limit cycle, which describes the macroscopic oscillations. We assume that this limit cycle does not undergo a bifurcation. Under this condition, the fluctuations around the limit cycle turn out to be of Gaussian character. Moreover, the phase of the oscillations diffuses along the limit cycle. This phase diffusion is the main mechanism which affects the periodicity of the oscillations in the presence of the molecular fluctuations.³⁵⁻³⁸ The Hamilton-Jacobi method allows us to determine quantitatively the magnitude of this phase diffusion, as explained below. A consequence of the phase diffusion is that the time autocorrelation functions of the chemical concentrations present oscillations which are exponentially damped. An explicit formula is obtained for the damping rate of the oscillations of the time autocorrelation functions. The inverse of this damping rate defines the correlation time of the oscillations of the biochemical clock.

In order to reach this result, we first define the (intensive) reaction rates

$$w_\rho(\mathbf{x}) \equiv \frac{1}{\Omega} W_\rho(\Omega \mathbf{x}) \quad (10)$$

corresponding to the six (extensive) transition rates $W_\rho(\mathbf{X})$ ($\rho = 1, 2, \dots, 6$). The stoichiometric coefficients of the six reactions are given by the matrix:

$$[\nu_\rho^i]_{i=1,2,3;\rho=1,2,\dots,6}$$

i/ρ	1	2	3	4	5	6
1	+1	-1	0	0	0	0
2	0	0	+1	-1	-1	+1
3	0	0	0	0	+1	-1

in terms of which the chemical master equation (6) takes the general form

$$\frac{d}{dt}P(\{X^i\},t) = \sum_{\rho=1}^r W_\rho(\{X^i - \nu_\rho^i\})P(\{X^i - \nu_\rho^i\},t) - W_\rho(\{X^i\})P(\{X^i\},t) \quad (12)$$

with $i = 1, 2, 3$.

A. Generalized Fokker-Planck equation

We express the population numbers $\{X^i\}$ in terms of the concentrations $x^i = X^i/\Omega$ and we introduce the probability density

$$\mathcal{P}(\mathbf{x},t) \equiv \Omega^3 P(\Omega x^1, \Omega x^2, \Omega x^3) \quad (13)$$

that the concentrations take the values $\mathbf{x} = (x^1, x^2, x^3)$ at the current time t .

The chemical master equation (12) can then be expanded in inverse powers of the extensivity parameter Ω to obtain the Fokker-Planck equation

$$\frac{\partial}{\partial t} \mathcal{P}(\mathbf{x},t) = - \sum_{j=1}^s \frac{\partial}{\partial x^j} [F^j(\mathbf{x}) \mathcal{P}(\mathbf{x},t)] + \frac{1}{\Omega} \sum_{j,k=1}^s \frac{\partial^2}{\partial x^j \partial x^k} [Q^{jk}(\mathbf{x}) \mathcal{P}(\mathbf{x},t)] \quad (14)$$

if the terms of order Ω^{-2} and higher are neglected. This approximation is justified if the limit cycle does not undergo a bifurcation. In Eq. (14), we have introduced the mean drifts of the concentrations

$$F^j(\mathbf{x}) = \sum_{\rho=1}^r \nu_\rho^j w_\rho(\mathbf{x}) \quad (15)$$

and the matrix of diffusivity

$$Q^{jk}(\mathbf{x}) = \frac{1}{2} \sum_{\rho=1}^r \nu_\rho^j \nu_\rho^k w_\rho(\mathbf{x}). \quad (16)$$

This diffusivity matrix is symmetric and non-negative. For the system defined in Table I, these quantities are given by

$$F^1 = w_1 - w_2,$$

$$F^2 = w_3 - w_4 - w_5 + w_6,$$

$$F^3 = w_5 - w_6,$$

$$Q^{11} = \frac{1}{2}(w_1 + w_2),$$

$$Q^{12} = Q^{21} = Q^{13} = Q^{31} = 0,$$

$$Q^{22} = \frac{1}{2}(w_3 + w_4 + w_5 + w_6),$$

$$Q^{23} = Q^{32} = \frac{1}{2}(-w_5 - w_6),$$

$$Q^{33} = \frac{1}{2}(w_5 + w_6) \quad (17)$$

in terms of the reaction rates (10) defined with the transition rates W_ρ of Table I.

B. Hamilton-Jacobi method

In the weak-noise limit $\Omega \rightarrow \infty$, the generalized Fokker-Planck equation (14) can be solved thanks to the Hamilton-Jacobi method by assuming that the probability density has the form^{31-34,38}

$$\mathcal{P}(\mathbf{x},t) = \exp \left[-\Omega \phi_0(\mathbf{x},t) - \phi_1(\mathbf{x},t) - \frac{\phi_2(\mathbf{x},t)}{\Omega} - \frac{\phi_3(\mathbf{x},t)}{\Omega^2} - \dots \right]. \quad (18)$$

Substituting in the generalized Fokker-Planck equation (14), we obtain the following Hamilton-Jacobi equation for the leading function ϕ_0 :

$$\frac{\partial \phi_0}{\partial t} + H \left(\mathbf{x}, \frac{\partial \phi_0}{\partial \mathbf{x}} \right) = 0 \quad (19)$$

with the special Hamiltonian

$$H(\mathbf{x},\mathbf{p}) = \sum_{j,k=1}^s Q^{jk}(\mathbf{x}) p_j p_k + \sum_{j=1}^s F^j(\mathbf{x}) p_j. \quad (20)$$

This Hamiltonian depends on the chemical concentrations \mathbf{x} as well as on canonically conjugated variables called momenta

$$\mathbf{p} \equiv \frac{\partial \phi_0}{\partial \mathbf{x}}. \quad (21)$$

Near the thermodynamic equilibrium, the function ϕ_0 would be interpreted as minus the excess entropy ΔS of the molecular fluctuations with respect to the state defined by the concentrations \mathbf{x} , $\phi_0 = -\Delta S$, if the extensive parameter is replaced with the Boltzmann constant, $\Omega = k_B$. In this case, the momenta could be identified as minus the thermodynamic forces:

$$p_i = \frac{\partial \phi_0}{\partial x^i} \approx - \frac{\partial \Delta S}{\partial x^i}. \quad (22)$$

In the weak-noise limit, the methods of Hamiltonian mechanics can thus be used to determine the solution of the generalized Fokker-Planck equation. This solution can be expressed in terms of the action

$$\phi_0(\mathbf{x},t) = \int \mathbf{p} \cdot d\mathbf{x} - H dt, \quad (23)$$

where the time integral is carried out over the trajectories of Hamilton's equations:

$$\dot{x}^i = + \frac{\partial H}{\partial p_i} = F^i(\mathbf{x}) + 2 \sum_{j=1}^s Q^{ij}(\mathbf{x}) p_j, \quad (24)$$

$$\dot{p}_i = - \frac{\partial H}{\partial x^i} = - \sum_{j=1}^s \frac{\partial F^j(\mathbf{x})}{\partial x^i} p_j - \sum_{j,k=1}^s \frac{\partial Q^{jk}(\mathbf{x})}{\partial x^i} p_j p_k,$$

We notice that the Hamilton equations (24) preserve the subspace of vanishing momenta $\mathbf{p}=0$. In this subspace, Hamilton's equations reduce to the equations of macroscopic chemical kinetics:

$$\dot{x}^i = F^i(\mathbf{x}) = \sum_{\rho=1}^r v_{\rho}^i w_{\rho}(\mathbf{x}) \quad \text{in } \mathbf{p}=0 \quad (25)$$

so that we here recover the macroscopic equations (1) according to the three first equations of Eq. (17) and the transition rates of Table I.

For a biochemical clock, the macroscopic system (25) admits a limit cycle or periodic attractor, which is a stable periodic solution of some prime period T . The prime period T is the smallest nontrivial number such that

$$\mathbf{x}(t+rT) = \mathbf{x}(t) \quad \text{for } r = \dots, -2, -1, 0, +1, +2, \dots \quad (26)$$

The stability of the limit cycle is characterized by linearizing the macroscopic equations (25)³⁹

$$\delta \dot{x}^i = \sum_{j=1}^s \frac{\partial F^i(\mathbf{x})}{\partial x^j} \delta x^j \quad \text{in } \mathbf{p}=0. \quad (27)$$

Since this system of equations is linear its general solution can be expressed in terms of a $s \times s$ matrix as

$$\delta \mathbf{x}(t) = \mathbf{M}(t) \cdot \delta \mathbf{x}(0) \quad \text{such as } \mathbf{M}(0) = \mathbf{1}. \quad (28)$$

At the prime period $t=T$, this matrix admits the eigenvalues $\{\Lambda_k\}$ and associated right- and left-eigenvectors according to

$$\begin{aligned} \mathbf{M}(T) \cdot \mathbf{e}_k &= \Lambda_k \mathbf{e}_k, \\ \mathbf{M}(T)^T \cdot \mathbf{f}_k &= \Lambda_k \mathbf{f}_k. \end{aligned} \quad (29)$$

The right- and left-eigenvectors satisfy the biorthonormality relations

$$\mathbf{e}_k \cdot \mathbf{f}_l = \delta_{kl}. \quad (30)$$

The eigenvalue corresponding to the direction of the flow is always equal to unity:

$$\Lambda_1 = 1, \quad \text{for } \mathbf{e}_1 = \dot{\mathbf{x}} = \mathbf{F}(\mathbf{x}_*) \quad (31)$$

if \mathbf{x}_* is a point chosen on the limit cycle. Since the limit cycle is supposed to be stable all the other eigenvalues satisfy the condition: $|\Lambda_k| < 1$ for $k \neq 1$. The corresponding Lyapunov exponents are defined by

$$\lambda_k \equiv \frac{1}{T} \ln |\Lambda_k|. \quad (32)$$

For a stable limit cycle, the Lyapunov exponents are ordered as $\lambda_1 = 0 > \lambda_2 \geq \lambda_3$. The dissipative character of the macroscopic system (25) manifests itself in the property that the time average of the divergence of the macroscopic system (25)—or equivalently the sum of Lyapunov exponents—is negative:

$$\lim_{t \rightarrow \infty} \frac{1}{t} \int_0^t \text{div } \mathbf{F} d\tau = \sum_k \lambda_k < 0, \quad (33)$$

where the integral is performed over a trajectory in $\mathbf{p}=0$ which converges toward the limit cycle.³⁹

Since the generalized Fokker-Planck equation (14) is independent of time, the Hamiltonian (20) does not depend on time so that Hamilton's equations (24) preserve a pseudo-energy

$$E = H(\mathbf{x}, \mathbf{p}). \quad (34)$$

According to Eq. (18), the quantity ϕ_0 has the physical units of the inverse of the extensivity parameter Ω , whereupon we infer from Eq. (23) that the pseudo-energy has the units of a rate (second^{-1}) divided by the units of the extensivity parameter Ω .

The action (23) can be expanded in a Taylor series around a point \mathbf{x}_* of the macroscopic limit cycle and around some repetition rT of the prime period T to get:

$$\begin{aligned} \phi_0(\mathbf{x}, t) \approx & \frac{1}{2} \frac{\partial^2 \phi_0(\mathbf{x}_*, rT)}{\partial t^2} (t-rT)^2 \\ & + \frac{1}{2} \frac{\partial^2 \phi_0(\mathbf{x}_*, rT)}{\partial \mathbf{x}^2} : (\mathbf{x} - \mathbf{x}_*)^2 \end{aligned} \quad (35)$$

neglecting higher-order terms. The terms of zeroth and first orders (as well as the cross term of second-order) can be shown to vanish because the limit cycle belongs to the invariant subspace $\mathbf{p}=0$ at vanishing pseudo-energy $E=0$ (see elsewhere⁴⁰). The second derivative of the action with respect to the time at some point $\mathbf{x} = \mathbf{x}_*$ can be shown⁴⁰ to be related to the derivative of the period with respect to the pseudo-energy according to

$$\frac{\partial^2 \phi_0(\mathbf{x}_*, rT)}{\partial t^2} = \frac{1}{r \left| \frac{\partial T}{\partial E} \right|}. \quad (36)$$

The sign can also be shown to be positive.⁴⁰

Accordingly, the probability density around some point \mathbf{x}_* of the limit cycle is given by

$$\begin{aligned} \mathcal{P}(\mathbf{x}, t) \sim \exp \left[- \frac{\Omega}{2r \left| \frac{\partial E T}{\partial E} \right|} (t-rT)^2 \right. \\ \left. - \frac{\Omega}{2} \frac{\partial^2 \phi_0(\mathbf{x}_*, rT)}{\partial \mathbf{x}^2} : (\mathbf{x} - \mathbf{x}_*)^2 \right] \end{aligned} \quad (37)$$

in the weak-noise limit $\Omega \rightarrow \infty$. In this limit, the probability density is thus of Gaussian character not only in the space of chemical concentrations \mathbf{x} but also in time around each repetition rT of the prime period.

C. Phase diffusion and consequences

As time increases, the probability distribution of the phase drifts and spreads along the time axis according to the following mean and variance:

$$\langle t \rangle \approx rT, \quad (38)$$

$$\langle (t-rT)^2 \rangle \approx \frac{r}{\Omega} \left| \frac{\partial E T}{\partial E} \right|. \quad (39)$$

We observe that the variance increases linearly with the repetition number r of the prime period, as expected for a pro-

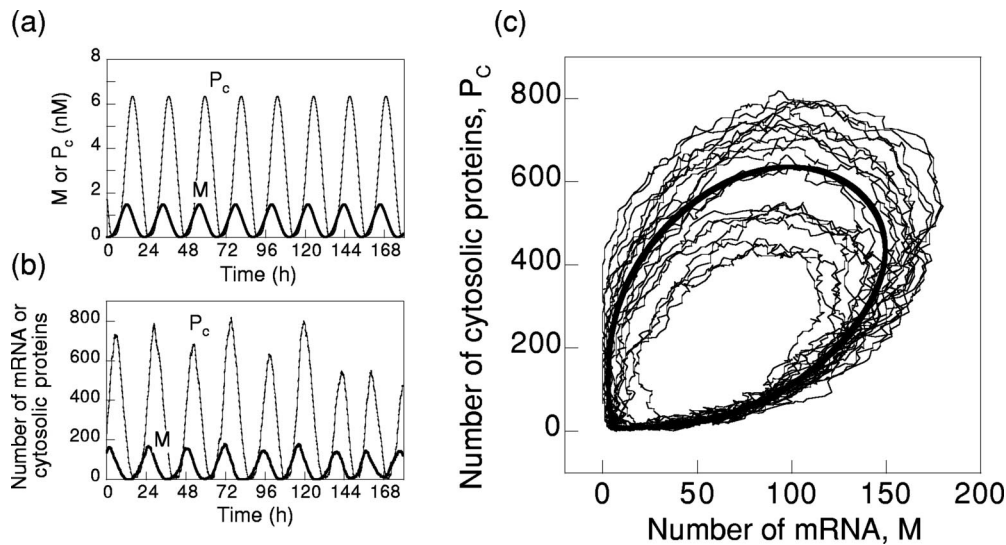


FIG. 2. Circadian oscillations given by the negative feedback model schematized in Fig. 1. (a) Oscillations of mRNA (M) and cytosolic clock protein (P_C) obtained, in the absence of noise, by numerical integration of the three deterministic kinetic equations (1) governing the time evolution of the model. The period is about 22h. The oscillations of P_N are similar to those of P_C and are not shown. (b) Corresponding oscillations generated by the model, in the presence of noise, for $\Omega = 100$ and $n = 4$. The data, expressed in numbers of molecules of mRNA (M) and of cytosolic protein (P_C), are obtained by stochastic simulations using the Gillespie algorithm. (c) Limit cycles represented as a projection into the (M, P_C) plane, corresponding to the deterministic (bold curve) and noisy (thin curves) oscillations. In this panel, the deterministic concentrations have been scaled to correspond to the number of molecules by multiplying the variables by $\Omega = 100$. The other parameter values are: $v_s = 0.5 \text{ nM h}^{-1}$, $k_l = 2.0 \text{ nM}$, $v_m = 0.3 \text{ nM h}^{-1}$, $k_m = 0.2 \text{ nM}$, $k_s = 2.0 \text{ h}^{-1}$, $v_d = 1.5 \text{ nM h}^{-1}$, $k_d = 0.1 \text{ nM}$, $k_1 = 0.2 \text{ h}^{-1}$, $k_2 = 0.2 \text{ h}^{-1}$.

cess of phase diffusion in the direction longitudinal to the limit cycle. The temporal diffusivity of the phase has the value

$$\lim_{r \rightarrow \infty} \frac{\langle (t - rT)^2 \rangle}{\langle t \rangle} \simeq \frac{|\partial_E T|}{\Omega T}. \quad (40)$$

As expected, the phase diffusion disappears in the noiseless limit $\Omega = \infty$.

If we defined the distribution of first-return times at a given value of a particular concentration x^i , Eq. (37) would suggest that the recurrences of the noisy clock are distributed randomly around the prime period T of the noiseless limit cycle. Indeed, according to Eq. (37) with $r = 1$, the distribution of the times of first return should be given by the Gaussian

$$\mathcal{P}(t) \simeq \frac{1}{\sigma \sqrt{2\pi}} \exp\left[-\frac{(t - T)^2}{2\sigma^2}\right] \quad (41)$$

in the limit $\Omega \rightarrow \infty$. If the effects of the fluctuations transverse to the limit cycle are neglected, the standard deviation of the distribution (41) is approximately given by

$$\sigma \simeq \frac{|\partial_E T|^{1/2}}{\Omega^{1/2}} \text{ for } \Omega \rightarrow \infty. \quad (42)$$

Furthermore, the phase diffusion directly affects the time autocorrelation functions of the chemical concentrations:

$$C(t) \equiv \langle x^i(t)x^i(0) \rangle. \quad (43)$$

Such time autocorrelation functions can be expressed in terms of the solution of the generalized Fokker-Planck equation (14) from some initial probability density $\mathcal{P}_0(\mathbf{x}_0)$ as

$$C(t) = \int x^i \mathcal{P}(\mathbf{x}, t; \mathbf{x}_0) x_0^i d\mathbf{x} d\mathbf{x}_0. \quad (44)$$

According to Eq. (37), such a probability density has a Gaussian dependence on time near each repetition rT of the prime period in the weak-noise limit. As time increases the probability density in Eq. (44) is therefore composed of a sum of Gaussian pulses. By the method of Laplace transforms, such a function can be shown⁴⁰ to present damped oscillations of the form

$$C(t) \simeq C_0 + |C_1| \exp\left(-\frac{t}{\tau}\right) \cos(\omega t + \alpha_1) \quad (t \rightarrow \infty) \quad (45)$$

with some coefficients C_0 , $|C_1|$ and a phase α_1 , which depend on the particular concentration entering the definition of the autocorrelation function (43).²⁹ However, the pulsation ω and the correlation time τ are independent of the particular concentration and are given by⁴⁰

$$\omega \simeq \frac{2\pi}{T}, \quad (46)$$

$$\tau \simeq \frac{2\Omega T}{|\partial_E T|} \left(\frac{T}{2\pi}\right)^2. \quad (47)$$

We introduce the half-life of the autocorrelation function as the time when the exponential envelope of the autocorrelation function (43) has decreased by 50%. Therefore, the half-life of the oscillations of the autocorrelation function is related to the correlation time by

$$\tau_{1/2} \equiv \tau \ln 2 \simeq \frac{\Omega \ln 2}{a} \quad (48)$$

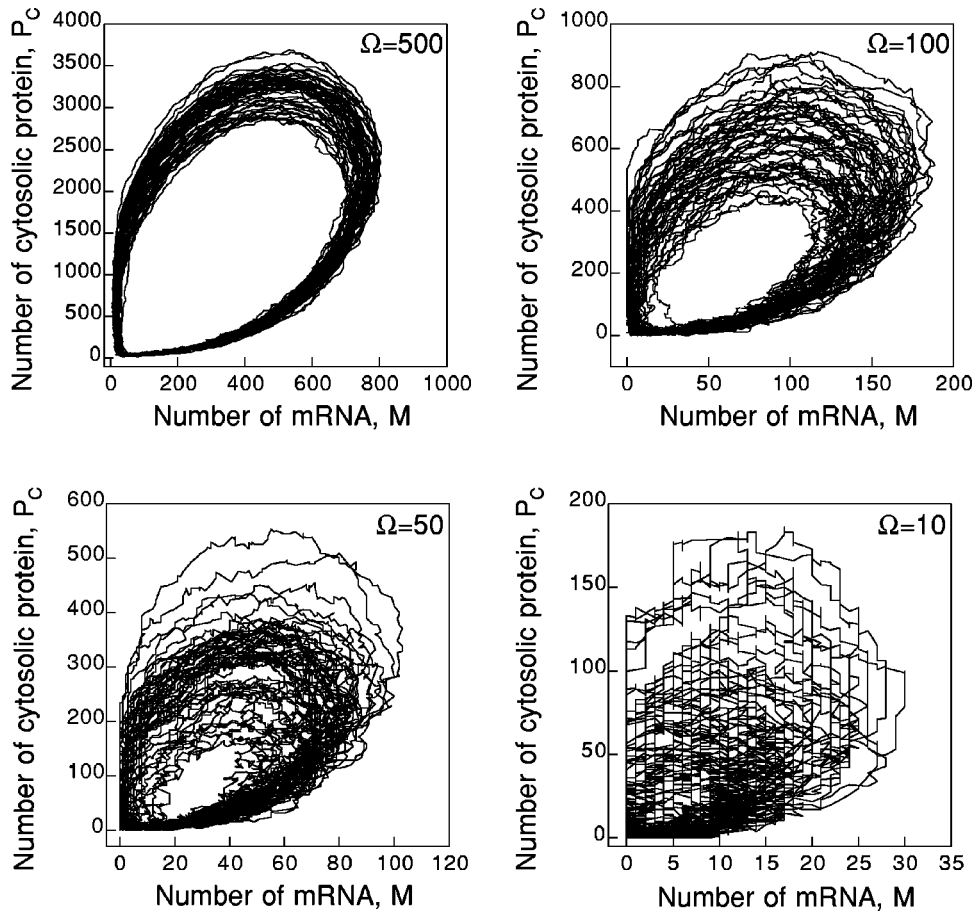


FIG. 3. Effect of the number of molecules on the robustness of the circadian oscillations. Shown are the noisy limit cycles, represented as a projection into the (M, P_c) plane, for parameter values $\Omega = 500, 100, 50,$ and 10 . The other parameter values are as in Fig. 2.

with the coefficient

$$a = \frac{|\partial_E T|}{2T} \left(\frac{2\pi}{T} \right)^2 \tag{49}$$

We observe that the half-life (48) increases proportionally to the size Ω of the system: the larger the system, the more correlated the oscillations are. We also notice that the half-life depends on the derivative of the period with respect to the pseudo-energy (34) of the Hamiltonian (20). This derivative can be calculated as explained in the Appendix.

The correlation time (47) provides an estimation of the minimum number of molecules required in the system for the oscillations to remain correlated in time over more than one prime period. Indeed, the autocorrelation function still presents a detectable recurrence as long as $\omega\tau > 1$, i.e., if the extensivity parameter is larger than a critical value given by

$$\Omega > \Omega_c = \frac{\pi |\partial_E T|}{T^2} \tag{50}$$

Since the number of molecules of species X^i is $X^i = \Omega x^i$ the maximum total number of molecules during one period of the oscillations is

$$N_{\max} = \Omega \left(\sum_{i=1}^s x^i \right)_{\max} \tag{51}$$

Therefore, in order for the oscillations to remain correlated, the total number of molecules which are present in the system should be larger than the critical value

$$N = \sum_{i=1}^s X^i > \Omega_c \left(\sum_{i=1}^s x^i \right)_{\max} \tag{52}$$

with Ω_c given by Eq. (50). The minimum total number of molecules (52) depends on the characteristic quantities of the limit cycle as well as on the diffusivity matrix (16) which enters in the expression of Ω_c given by Eq. (50) because the pseudo-energy E depends on the diffusivity by Eqs. (20) and (34). On the other hand, the prime period T and the maximum of the sum of concentrations depend only on the mean drifts $\mathbf{F}(\mathbf{x})$ of the macroscopic kinetic equations (25).

We should here remark that the biochemical oscillations can still be observable for $\Omega < \Omega_c$ below the critical value (50). However, the recurrence (or first-return) times are then widely distributed in time with a standard deviation (42) larger than the period:

$$\sigma > T \text{ if } \Omega < \frac{\Omega_c}{\pi} \tag{53}$$

V. RESULTS AND DISCUSSION

In this section, we present the results of the simulation of the biochemical clock with Gillespie algorithm and we compare with the predictions of the theory exposed in Sec. IV.

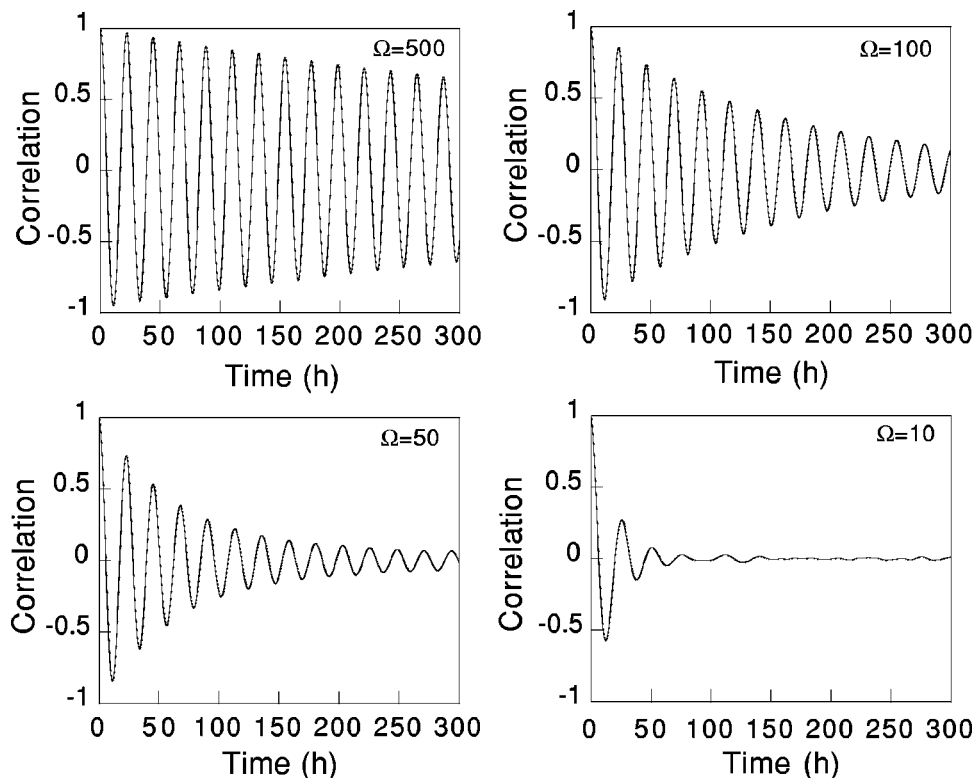


FIG. 4. Time evolution of the autocorrelation function for different values of the extensivity parameter Ω corresponding to oscillations shown in Fig. 3. When Ω is decreased, the loss of correlations, which corresponds to the damping of the correlation function, is more rapid. The other parameter values are as in Figs. 2 and 3.

A. Comparison between deterministic and stochastic oscillations

For a given set of parameters values, the numerical integration of the deterministic kinetic equations (1) of the model presents sustained oscillations corresponding to a limit cycle with a period of about 22h [Fig. 2(a)]. Similar oscillations are obtained by stochastic simulations of the model using the Gillespie method explained in Sec. III [Fig. 2(b)]. These figures show that the stochastic oscillations present fluctuations around the deterministic limit cycle. The amplitude of these fluctuations depends on the number of molecules present in the system. In the phase space, these fluctuations correspond to a set of trajectories around the deterministic limit cycle [Fig. 2(c)]. If the number of molecules in the system is too low the fluctuations take over the regular oscillations and the system loses its periodicity.

In the Gillespie method, the extensivity parameter Ω controls the total number of molecules that can be present in the system. For values of Ω of the order of 500, the trajectories in the phase space are densely packed around the deterministic limit cycle (Fig. 3, with $\Omega = 500$). Upon decreasing Ω (i.e., when lowering number of molecules), the trajectories expand and explore a larger area of the phase space. The dispersion of the trajectories in the phase space is not homogeneous but depends on the characteristics of the limit cycle. The phase portraits show regions of contraction and others of expansion of phase-space volumes (Fig. 3). At very low values of Ω (of the order of 10) the structure of the limit cycle is nearly completely lost and the system produces widely irregular oscillations (Fig. 3, with $\Omega = 10$).

B. Half-life of the autocorrelation functions

The effect of the molecular noise on the robustness of the oscillations can be characterized by the autocorrelation functions depicted in Fig. 4. When $\Omega = 500$, the autocorrelation function presents oscillations which are slowly damped. In this case, the system would keep its periodicity during several days: The half-life of the correlation is about 440h (i.e., 20 days). If Ω is decreased, we observe that the damping of the correlation function becomes more pronounced. Consequently, when the number of molecules present in the system is lowered, the effect of the fluctuations is higher on the periodicity of the system. For $\Omega = 100$, the half-life of the correlation is about 100h (i.e., 4 days), at $\Omega = 50$ the half-life is only about 48h, and at $\Omega = 10$, correlations are rapidly lost in less than a period of the oscillations. This loss of correlation is mainly due to the diffusion of the phase.^{35–38}

We emphasize that, in agreement with the theoretical discussion in Sec. IV, the noisy system still presents relatively well-defined oscillations [Fig. 2(b), with $\Omega = 100$] with a mean period very close to the deterministic period. Nevertheless, the memory of the initial conditions and, especially, of the phase, is progressively lost as time increases because of phase diffusion. The lower is the number of molecules present in the system, the more rapid is the loss of the initial condition memory.

As explained in Sec. IV, we expect a linear relationship between Ω and the half-life of the autocorrelation function according to Eq. (48). The values of the quantities entering into the coefficient (49) are given in Table II. On the other hand, we have computed the half-life for varying values of Ω

TABLE II. Numerical values for the period T , the derivative $\partial T/\partial E$, and the Lyapunov exponents $\{\lambda_1, \lambda_2, \lambda_3\}$ vs the Hill coefficient n for the model of Table I with the parameters: $v_s=0.5 \text{ nM h}^{-1}$, $k_f=2.0 \text{ nM}$, $v_m=0.3 \text{ nM h}^{-1}$, $k_m=0.2 \text{ nM}$, $k_s=2.0 \text{ h}^{-1}$, $v_d=1.5 \text{ nM h}^{-1}$, $k_d=0.1 \text{ nM}$, $k_1=0.2 \text{ h}^{-1}$, $k_2=0.2 \text{ h}^{-1}$. The unit of time is the hour (h).

n	T	$\partial T/\partial E$	λ_1	λ_2	λ_3
1.0	30.926	-2107.3	0.0	-0.020	-0.532
1.5	27.077	-751.8	0.0	-0.074	-0.662
2.0	25.029	-537.3	0.0	-0.118	-0.806
2.5	23.774	-460.7	0.0	-0.160	-0.925
3.0	22.945	-430.0	0.0	-0.198	-1.018
3.5	22.372	-417.2	0.0	-0.231	-1.090
4.0	21.962	-412.6	0.0	-0.261	-1.147
4.5	21.661	-412.8	0.0	-0.286	-1.191
5.0	21.435	-414.2	0.0	-0.309	-1.226
5.5	21.261	-416.8	0.0	-0.328	-1.253
6.0	21.124	-420.4	0.0	-0.346	-1.275
6.5	21.016	-421.6	0.0	-0.361	-1.292
7.0	20.927	-424.0	0.0	-0.374	-1.306
7.5	20.854	-425.7	0.0	-0.387	-1.317
8.0	20.792	-427.3	0.0	-0.397	-1.326

by stochastic simulation. Figure 5 shows the perfect agreement between the simulations and the theoretical prediction (48) with the coefficient (49). Indeed, by linear regression, we find

$$\frac{\tau_{1/2}}{T} = 0.0411 \Omega \quad (54)$$

in the case of the Hill coefficient $n=4$, which is in excellent agreement with the theoretical value of

$$\frac{\tau_{1/2}}{T} = 0.04105 \Omega \quad (55)$$

according to the formula (49).

We have also studied the influence of the Hill coefficient, n , on the robustness of the oscillations. Figure 6 depicts the behavior of the half-life for a system with $\Omega = 100$ as a function of the Hill coefficient n , i.e., of the degree of cooperativity of the inhibition in the production of the clock mRNA. We observe in Fig. 6 that the half-life

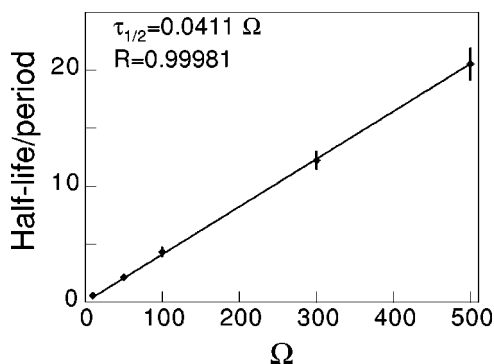


FIG. 5. The half-life of the autocorrelation function vs the extensivity parameter Ω in the case of the Hill coefficient $n=4$. The black points are the averages measured on 20 simulations, each over 50 000 hours (i.e., about 2200 periods) and vertical bars are standard deviations with a confidence interval of 95%. The dependence is linear as predicted by Eq. (48). A linear regression gives a slope of 0.0411 (solid line) with a correlation coefficient $R=0.99981$.

rapidly increases as the Hill coefficient increase from $n=1$ to $n=2$. A maximum is reached between $n=2$ and $n=3$. The half-life then decreases to a moderately high value for higher values $n>3$ of the Hill coefficient. This behavior, which is explained here below, has also been observed for more detailed models of circadian rhythms.¹¹ Accordingly, for a given value of Ω , the limit cycle is more robust with respect to the molecular noise when the system has a Hill coefficient larger than $n=1$. The cooperativity of the inhibition is thus a factor that allows the systems to resist to the molecular noise.

Several factors explain the increase of the correlation time of the biochemical clock in the presence of cooperativity. When the Hill coefficient takes the unit value $n=1$ the limit cycle is of harmonic type and located in the middle of the phase space [Fig. 7(a)]. In contrast, the anharmonicity and the stiffness of the limit cycle increases with the Hill coefficient. The limit cycle then becomes of relaxation type

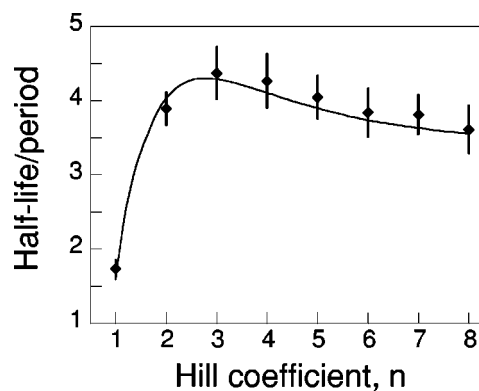


FIG. 6. Half-life of autocorrelations vs the degree of cooperativity characterized by the Hill coefficient n for $\Omega=100$. The solid line corresponds to the theoretical curve given by Eqs. (48) and (49). The black points are the averages measured on 20 simulations, each over 50 000 hours (i.e., about 2200 periods) and vertical bars are standard deviations with a confidence interval of 95%. The parameter values are the same as in Fig. 2. The maximum results from the combined effect of the decrease of the period [see Fig. 7(b)] and the increase of $\partial E T$ (see Fig. 8) as n increases (see text).

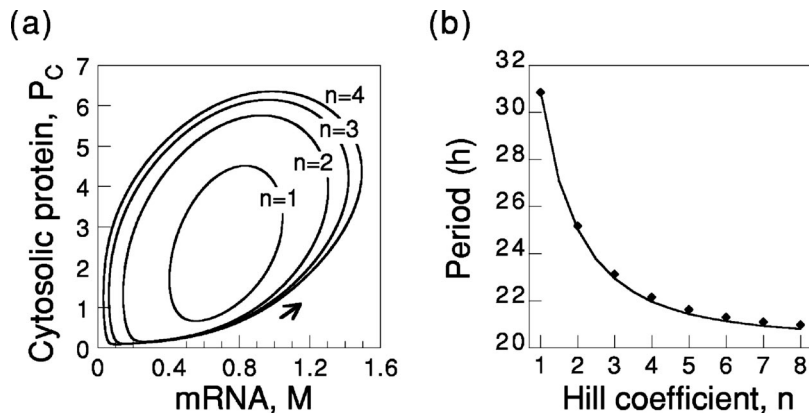


FIG. 7. (a) Phase portrait of the limit cycle of the macroscopic system for varying values of the Hill coefficient n . (b) Period of the oscillations vs the degree of cooperativity given by Hill's coefficient n for $\Omega = 100$. The black points are the means of the period measured on 20 simulations each of about 2200 periods (as in Fig. 6). The solid line corresponds to the values of the period calculated by integrating the deterministic kinetic equations. The parameter values are the same as in Fig. 2.

and part of it evolves at low concentrations near the axes of the phase space [Fig. 7(a)]. Moreover, Fig. 7(b) shows that the period of the limit cycle varies more rapidly for $n=1$ than for higher values of Hill's coefficient, which is a further evidence of the fragile character of the oscillations when $n=1$.

According to Eq. (49), the main parameter which controls the half-life of the autocorrelation function is the derivative $\partial_E T$ of the period with respect to the pseudo-energy. This quantity is plotted as a function of the Hill coefficient in Fig. 8. We observe in this figure that this quantity increases very much between $n=1$ and $n=2$, reaches an unpronounced maximum near $n=4$, and tends to a nearly constant value at higher values of n when the limit cycle becomes of relaxation type. Equations (48) and (49) show that the half-life behaves as $\tau_{1/2} \sim \Omega T^3 / |\partial_E T|$. Accordingly, the maximum of the half-life around $n \approx 3$ observed in Fig. 6 results from the combined effect of the rapid increase of $\partial_E T$ between $n=1$ and $n=2$ (Fig. 8) and of the slow decrease of the period T which persists for $n > 3$ [Fig. 7(b)]. We notice that the maximum of the half-life occurs where $\partial_n \tau_{1/2} = 0$, i.e., where $3 \partial_n T / T = \partial_n |\partial_E T| / |\partial_E T|$, which explains that the maximum of $\tau_{1/2}$ does not coincide with the maximum of $\partial_E T$ where $\partial_n |\partial_E T| = 0$.

C. Distribution of the first-return times

Even in the presence of noise, we see in Fig. 2(b) that the oscillations of the biochemical clock repeat themselves in spite of the decay of the autocorrelation function depicted in Fig. 4. Indeed, the autocorrelation functions measure the correlation between an event at a given time t_0 and another event at a later time $t_0 + t$. The phase diffusion tends to destroy these correlations, but the oscillations remain. Accordingly, it is interesting to study a further quantity that would describe the repetitive and sustained character of the noisy oscillations. Such a quantity is the probability distribution of the times of first return of one of the concentrations (or equivalently one of the numbers of molecules) to its average value. The theory of Sec. IV predicts that this distribution should be Gaussian of the form (41) with an average close to the deterministic period $\mu \approx T$ and a standard deviation given by Eq. (42) in the weak-noise limit $\Omega \rightarrow \infty$.

Figure 9(a) depicts the histogram of the first-return times, which shows that the distribution remains well-

centered around the deterministic period. The standard deviation σ is depicted in Fig. 9(b) and we find by linear regression that

$$\sigma = \frac{20.1}{\Omega^{1/2}} \quad (56)$$

which is in good agreement with the theoretical value predicted by Eq. (42)

$$\sigma = \frac{20.3}{\Omega^{1/2}} \quad (57)$$

in the case $n=4$ (cf. Table II).

These results confirm that the oscillations may be dephased by the phase diffusion but that they remain sustained even in the presence of molecular fluctuations. The first-return times are better and better centered on the deterministic period as the system becomes macroscopic.

D. Effect of the attractivity of the limit cycle

We have also observed that the Lyapunov exponents of the limit cycle become more negative for increasing values of the Hill coefficient n . Hence, the limit cycle attracts more strongly the trajectories when the Hill coefficient is higher (Fig. 10). As a consequence, the contractivity of phase-space

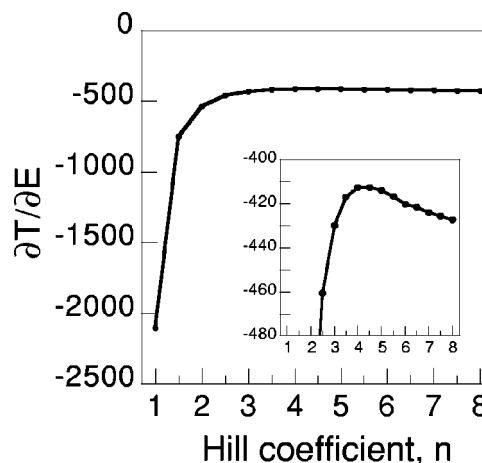


FIG. 8. Derivative $\partial T / \partial E$ of the period of the oscillations with respect to the pseudo-energy E vs the Hill coefficient n . The parameter values are the same as in Fig. 2.

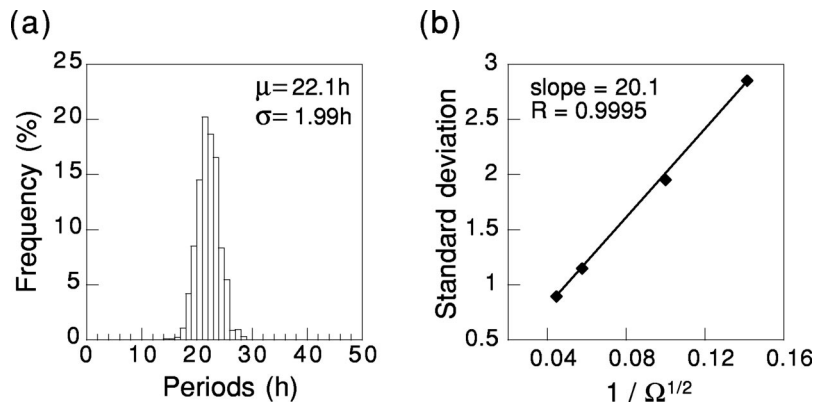


FIG. 9. (a) Histogram of the times of first return of the number M of mRNA to its average value, in the case $n=4$ and $\Omega=100$. The histogram is obtained from one simulation over 50 000 hours (i.e., about 2200 periods). (b) Standard deviation of these first-return times vs $\Omega^{-1/2}$ in the case $n=4$. The black points are the averages measured on 20 simulations, each over 50 000 hours.

volumes [which is characterized by the divergence of the macroscopic equations according to Eq. (33)] also increases with n .

This divergence is the main factor influencing the dispersion of the trajectories around the limit cycle [Figs. 11(c),11(d)]. The contraction of nearby trajectories is maximal when the divergence of the flow near the limit cycle is minimal. Around the minimum of divergence the trajectories are compressed in the phase space. Figure 11(c) shows the divergence along the limit cycle during one period. Figure 11(d) shows the limit cycle in the phase space plane (M, P_C) on which the values of the divergence have been reported. The minimum of divergence (-9.54) corresponds to the lower left corner of the (M, P_C) plane where most of the contraction of the trajectories occurs (Fig. 3). It corresponds to a low number of molecules present in the system. The divergence is minimal at the minima of mRNA (M) and cytosolic protein (P_C) number of molecules [Fig. 11(a) and Figs. 3(a)–3(d)]. Figure 12 depicts the divergence and the speed versus the Hill coefficient n .

We observe in Fig. 3 and Fig. 11 that the spreading of the trajectories occurs when the chemical reactions of the biological clock are producing molecules.

We also notice that the speed along the limit cycle presents its minimum when the divergence is minimal. It presents a second local minimum corresponding to the maximum reached by the nuclear proteins during the oscillations. The speed along the limit cycle is thus maximal when the system is producing or destroying molecules, i.e. when the number of molecules is rapidly rising or decreasing. The variation of speed along the limit cycle is correlated to the phase relationship between the variables. First, the number of mRNA molecules is slowly rising due to the absence of repression. The mRNA molecules induce the rapid synthesis of cytosolic proteins which are progressively transported into the nucleus where they exert their repression activity. Second, the speed reaches its maximum and starts to decrease because the number of nuclear proteins is at its maximum repressing the transcription and hence the proteins synthesis. Third, the speed rise again while the system is rapidly degrading the cytosolic and nuclear proteins.

However, the speed does not play the main role in the spreading of the trajectories, which is mainly determined by the divergence of the macroscopic equations and therefore by the local attractivity of the limit cycle. This attractivity in-

creases with the Hill coefficient together with the general increase of the correlation time (or half-life) of the oscillations. We can here conclude that the cooperativity tends to increase the attractivity of the limit cycle, which also contributes to the robustness of the oscillations.

VI. CONCLUSIONS AND PERSPECTIVES

In this paper, we have studied the influence of molecular fluctuations on biochemical clocks and, in particular, on circadian rhythms. Since these biochemical clocks take place inside a single cell, the low number of molecules involved at the subcellular level has the consequence that the molecular fluctuations can play a significant role. In order to address this question we have here studied the effect of these fluctuations on a simple model of the circadian rhythm.

In the presence of molecular fluctuations, the time evolution of the chemical populations obeys a stochastic process which we have modeled as a birth-and-death process described by the chemical master equation by Nicolis and co-workers.^{24–26} The reactions are supposed to take place homogeneously within each of the two intracellular compartments of the model, namely, the nucleus and the cytosol. This process has been simulated by an algorithm proposed by Gillespie.^{27,28} Because of the molecular noise, the chemical concentrations are randomly distributed around the limit cycle of the corresponding macroscopic system. Moreover,

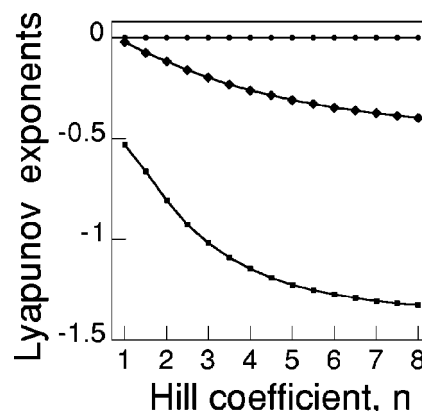


FIG. 10. Lyapunov exponents $\lambda_1=0>\lambda_2>\lambda_3$ vs the Hill coefficient n . These points have been calculated by Eq. (32) with the same parameter values as in Fig. 2.

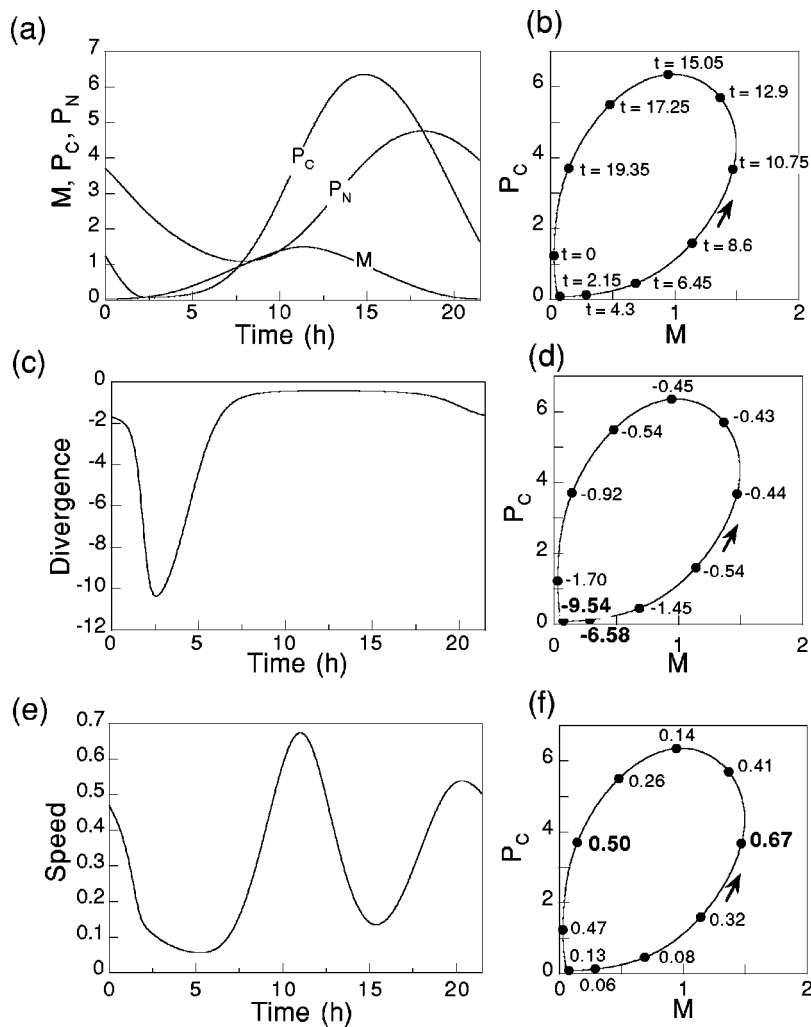


FIG. 11. (a) Deterministic oscillations for the three variables M , P_C and P_N over one period is shown with the corresponding limit cycle [panel (b)]. Time 0 is defined as the minimum of M . The parameter values are the same as in Fig. 2. (c) Divergence and (e) speed along one period, panels (d) and (f) show the limit cycles on which the values of the divergence and the speed have been reported at different time.

the noise induces a phase diffusion, which causes a loss of correlation between the successive oscillations which nevertheless continue to be sustained.^{35–38} The loss of correlation reduces the robustness of the biochemical clock. As a vehicle of our study we have here considered the minimal model (1) but we should mention that stochastic simulations of extended versions of this model lead to similar results.^{11,12}

The robustness of the oscillations can be characterized by different methods: phase portraits, autocorrelation functions, probability distribution of first-return times, global and local stability analyses. First of all, we have computed the autocorrelation functions, which measure the statistical correlation between successive oscillations. Our simulations show that such autocorrelation functions present oscillations which are exponentially damped. The damping rate of the exponential envelope of the autocorrelation function defines a half-life or time of correlation between successive oscillations. This half-life is directly determined by the phase diffusion and we have been able to obtain a precise and quantitative theoretical prediction for the half-life of the autocorrelation function.

With the Hamilton-Jacobi method, we have inferred that the half-life of the autocorrelation functions, as well as the inverse of the variance of the probability distribution of first-return times, are inversely proportional to the quantity $|\partial_E T|$

which is the derivative of the period of the oscillations with respect to the pseudo-energy E of the Hamilton-Jacobi method [cf. Eqs. (42) and (48)–(49)]. Our results lead to the general prediction that the smaller the quantity $|\partial_E T|$ is the greater the robustness of the oscillator is. Besides, we notice that the quantity $|\partial_E T|$ takes values which are specific to the kinetic scheme and the parameter values of the model under study. For the kinetic scheme (1), we have here shown that the quantity $|\partial_E T|$ decreases significantly in the presence of cooperativity in the inhibition of the production of clock mRNA by the nuclear clock protein. The theoretical predictions have been found to be in excellent agreement with the numerical simulation based on Gillespie's method.

These results show that the half-life very much depends on the nonlinearity of the biochemical oscillator and, especially, on the Hill coefficient which characterizes the cooperativity. Without cooperativity, the limit cycle appears to be fragile with a highly variable period and a low attractivity. With cooperativity, the nonlinearity and the stiffness of the kinetics increases and the limit cycle becomes of relaxation type.

Relaxation-type limit cycles turn out to be much less sensitive to molecular noise and to be much more attractive, as evidenced by the behavior of the quantity $|\partial_E T|$ and of the Lyapunov exponents. A local analysis of the stability and, in

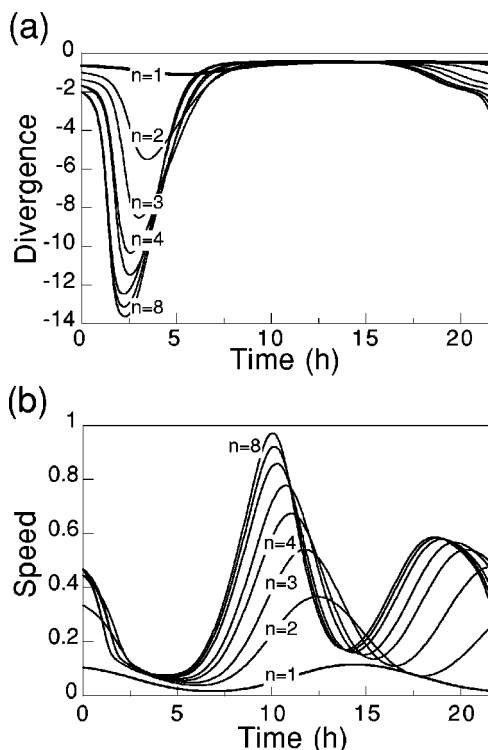


FIG. 12. (a) Divergence and (b) speed along one period of the oscillations for values of the degree of cooperativity n ranging from 1 to 8. Note that the period increases as n decreases [Fig. 7(b)]. The other parameter values are the same as in Fig. 2. When n is increased the oscillations become more anharmonic.

particular, of the divergence of trajectories around the limit cycle, confirms the importance of the attractivity in the robustness of the oscillations.

Here, we should mention that the sensitivity to molecular noise is enhanced when the kinetic parameters are close to a point of Hopf bifurcation. Indeed, the Hopf bifurcation is known to be the origin of the oscillations and a limit cycle weakens its attractivity in the vicinity of a Hopf bifurcation.^{25,39} Accordingly, the robustness of the oscillations would be affected near a Hopf bifurcation as it has been shown by numerical simulations done with extended versions of the core model presented here.⁴¹ In this regard, we point out that the present results are obtained for parameter values far from the Hopf bifurcation points. Since, for the present model, the domain of oscillation is relatively large in the parameter space, our results would remain valid for significant changes in the parameter values. The lack of robustness reported in Ref. 10 on a related extended version of the present core model may be due, as shown in Ref. 11, to smaller values of some parameters that bring the system very close to the Hopf bifurcation point.

Our results also show that a biochemical clock requires a minimum number of molecules involved in its reacting network in order to be able to keep the time and act as a clock [cf. Eq. (52)]. This conclusion is of particular importance in our understanding of self-organization in biological systems because it gives a fundamental limit to the proper functioning of regulatory reaction networks under nonequilibrium conditions. In this perspective, nonequilibrium self-

organization appears as a possible emerging property beyond a critical minimum size. Self-organization below such a critical size is nevertheless possible in the form of equilibrium structures by mechanisms such as the self-assembly of supramolecular structures, which can be involved in nonequilibrium functions as in the case of molecular motors.

Another important aspect is the robustness of the biochemical clocks under an external periodic forcing. The study of Ref. 30 has shown that a periodic forcing can induce a phase locking of the clock by the external signal. The sensitivity of this phase locking with respect to the molecular noise can be quantitatively studied by methods similar to the ones developed in the present work.¹¹

In conclusion, we have here developed quantitative methods which allow us to address the question of the robustness of biochemical clocks under the influence of the molecular noise. We think that these methods can be applied to further systems and will contribute to clarify the role of molecular noise in circadian rhythms and other chemical or biochemical clocks.

ACKNOWLEDGMENTS

The authors thank Professors A. Goldbeter and G. Nicolis for support and encouragement in this research, as well as F. Baras for fruitful discussions. D.G. gratefully acknowledges the financial support of the Foundation D. & A. Van Buuren. P.G. is financially supported by the National Fund for Scientific Research (F. N. R. S. Belgium). This research is supported, in part, by the Interuniversity Attraction Pole program of the Belgian Federal Office of Scientific, Technical and Cultural Affairs and by the National Fund for Scientific Research (F. N. R. S. Belgium).

APPENDIX: METHOD OF CALCULATION OF $\partial T/\partial E$

The derivative $\partial T/\partial E$ can be calculated by linearizing Hamilton's equations (24) around the limit cycle in the invariant subspace $\mathbf{p}=0$:

$$\begin{aligned}\delta\dot{\mathbf{x}} &= \frac{\partial \mathbf{F}}{\partial \mathbf{x}} \cdot \delta\mathbf{x} + 2\mathbf{Q} \cdot \delta\mathbf{p}, \\ \delta\dot{\mathbf{p}} &= -\frac{\partial \mathbf{F}^T}{\partial \mathbf{x}} \cdot \delta\mathbf{p}\end{aligned}\quad (\text{A1})$$

with $\mathbf{F} = \{F^j\}_{j=1}^s$ and $\mathbf{Q} = \{Q^{jk}\}_{j,k=1}^s$.

Outside the invariant subspace $\mathbf{p}=0$, we expect that the limit cycle extends into another periodic solution of slightly shifted period $T + \delta T$ such that

$$\begin{aligned}\mathbf{x}(T + \delta T) &= \mathbf{x}(0), \\ \mathbf{p}(T + \delta T) &= \mathbf{p}(0)\end{aligned}\quad (\text{A2})$$

at the pseudo-energy

$$\delta E = H = \mathbf{F}[\mathbf{x}(0)] \cdot \delta\mathbf{p}(0). \quad (\text{A3})$$

The perturbations with respect to the limit cycle in $\mathbf{p}=0$ are therefore given by the coupled equations

$$\begin{cases} \delta\dot{\mathbf{x}}(T) + \dot{\mathbf{x}}(T)\delta T = \delta\mathbf{x}(0) \\ \delta\dot{\mathbf{p}}(T) + \dot{\mathbf{p}}(T)\delta T = \delta\mathbf{p}(0) \end{cases} \quad (\text{A4})$$

with $\dot{\mathbf{x}}(T) = \dot{\mathbf{x}}(0) = \mathbf{F}[\mathbf{x}(0)]$ and $\dot{\mathbf{p}}(T) = \dot{\mathbf{p}}(0) = 0$ for the limit cycle in $\mathbf{p} = 0$. The solution of the linearized equations (A1) are given by

$$\begin{cases} \delta\mathbf{x}(T) = \mathbf{M}(T) \cdot \delta\mathbf{x}(0) + \mathbf{N}(T) \cdot \delta\mathbf{p}(0) \\ \delta\mathbf{p}(T) = \mathbf{M}(T)^{-1 \text{ T}} \cdot \delta\mathbf{p}(0) \end{cases}, \quad (\text{A5})$$

where $\mathbf{M}(T)$ is the matrix introduced in Eq. (28) while

$$\mathbf{N}(T) = 2\mathbf{M}(T) \cdot \int_0^T \mathbf{M}(\tau)^{-1} \cdot \mathbf{Q}[\mathbf{x}(\tau)] \cdot \mathbf{M}(\tau)^{-1 \text{ T}} d\tau. \quad (\text{A6})$$

The initial perturbations on the limit cycle can be expanded in the bases of the right- and left-eigenvectors (29) of the matrix $\mathbf{M}(T)$ as

$$\delta\mathbf{x}(0) = \sum_k \delta\xi_k \mathbf{e}_k \quad \text{and} \quad \delta\mathbf{p}(0) = \sum_k \delta\pi_k \mathbf{f}_k. \quad (\text{A7})$$

Since the eigenvectors are biorthonormal and $\mathbf{e}_1 = \mathbf{F}[\mathbf{x}(0)]$, we obtain from Eq. (A3) that $\delta\pi_1 = \delta E$. By the second lines of Eqs. (A4) and (A5), we moreover get that $\delta\pi_k = 0$ if $\Lambda_k \neq 1$. Similarly, the first lines of Eqs. (A4) and (A5) give an equation for δT and $\delta\xi_k$. Taking the scalar product with \mathbf{f}_1 and using the biorthonormality (30), we obtain δT in terms of δE and thus

$$\frac{\delta T}{\delta E} = - \frac{\mathbf{f}_1^{\text{T}} \cdot \mathbf{N}(T) \cdot \mathbf{f}_1}{\mathbf{f}_1 \cdot \mathbf{e}_1}. \quad (\text{A8})$$

This expression can be rewritten as

$$\frac{\delta T}{\delta E} = - \frac{\mathbf{f}_1 \cdot \delta\tilde{\mathbf{x}}(T)}{\mathbf{f}_1 \cdot \mathbf{e}_1}, \quad (\text{A9})$$

where $\delta\tilde{\mathbf{x}}(T) = \mathbf{N}(T) \cdot \mathbf{f}_1$ is solution of the linearized system (A1) from the special initial conditions $\delta\tilde{\mathbf{x}}(0) = 0$ and $\delta\tilde{\mathbf{p}}(0) = \mathbf{f}_1$ [see Eq. (A5)].

In this way, we can obtain the derivative of the period with respect to the pseudo-energy in terms of the matrix $\mathbf{M}(T)$ of stability of the limit cycle and its right- and left-eigenvectors associated with the direction of the flow along which the phase diffusion occurs.

The method presented in this Appendix is related to the method of Ref. 38 based on Floquet theory. The present method does not use Floquet theory and can be implemented with a numerical integrator of ordinary differential equations. In the present paper, the numerical integrations have been carried out with a fourth-order Runge-Kutta integrator.

- ¹C. J. Morton-Firth and D. Bray, *J. Theor. Biol.* **192**, 117 (1998).
- ²H. H. McAdams and A. Arkin, *Proc. Natl. Acad. Sci. U.S.A.* **94**, 814 (1997).
- ³A. Arkin, J. Ross, and H. H. McAdams, *Genetics* **149**, 1633 (1998).
- ⁴J. Hasty, J. Pradines, M. Dolnik, and J. J. Collins, *Proc. Natl. Acad. Sci. U.S.A.* **97**, 2075 (2000).
- ⁵M. Thattai and A. van Oudenaarden, *Proc. Natl. Acad. Sci. U.S.A.* **98**, 8614 (2001).
- ⁶J. C. Dunlap, *Cell* **96**, 271 (1999).
- ⁷M. W. Young, *Trends Biochem. Sci.* **25**, 601 (2000).
- ⁸D. K. Welsh, D. E. Logothetis, M. Meister, and S. M. Reppert, *Neuron* **14**, 697 (1995).
- ⁹E. D. Herzog, J. S. Takahashi, and G. D. Block, *Nat. Neurosci.* **1**, 708 (1998).
- ¹⁰N. Barkai and S. Leibler, *Nature (London)* **403**, 267 (2000).
- ¹¹D. Gonze, J. Halloy, and A. Goldbeter, *Proc. Natl. Acad. Sci. U.S.A.* **99**, 673 (2002).
- ¹²D. B. Forger and C. S. Peskin, *Mechanism Responsible for Immunity to Molecular Noise in Circadian Clocks* (preprint, Courant Institute of Mathematical Sciences, 2001).
- ¹³A. Goldbeter, *Proc. R. Soc. London, Ser. B* **261**, 319 (1995).
- ¹⁴A. Goldbeter, *Biochemical Oscillations and Cellular Rhythms: The Molecular Bases of Periodic and Chaotic Behaviour* (Cambridge University Press, Cambridge, UK, 1996).
- ¹⁵J.-C. Leloup, D. Gonze, and A. Goldbeter, *J. Biol. Rhythms* **14**, 433 (1999).
- ¹⁶H. Zeng, Z. Qian, M. P. Myers, and M. Rosbash, *Nature (London)* **380**, 129 (1996).
- ¹⁷J.-C. Leloup and A. Goldbeter, *J. Biol. Rhythms* **13**, 70 (1998).
- ¹⁸N. R. Glossop, L. C. Lyons, and P. E. Hardin, *Science* **286**, 766 (1999).
- ¹⁹J. Blau, *Semin. Cell Dev. Biol.* **12**, 287 (2001).
- ²⁰K. Lee, J. J. Loros, and J. C. Dunlap, *Science* **289**, 107 (2000).
- ²¹M. Merrow, T. Roenneberg, G. Macino, and L. Franchi, *Semin. Cell Dev. Biol.* **12**, 279 (2001).
- ²²H. R. Ueda, M. Hagiwara, and H. Kitano, *J. Theor. Biol.* **210**, 401 (2001).
- ²³J.-C. Leloup and A. Goldbeter (unpublished).
- ²⁴G. Nicolis, *J. Stat. Phys.* **6**, 195 (1972).
- ²⁵G. Nicolis and I. Prigogine, *Self-Organization in Nonequilibrium Systems* (Wiley, New York, 1977).
- ²⁶G. Nicolis and M. Malek Mansour, *Prog. Theor. Phys. Suppl.* **64**, 249 (1978).
- ²⁷D. T. Gillespie, *J. Comput. Phys.* **22**, 403 (1976).
- ²⁸D. T. Gillespie, *J. Phys. Chem.* **81**, 2340 (1977).
- ²⁹G. Nicolis and P. Gaspard, *Chaos, Solitons Fractals* **4**, 41 (1994).
- ³⁰D. Gonze and A. Goldbeter, *J. Stat. Phys.* **101**, 649 (2000).
- ³¹R. Kubo, K. Matsuo, and K. Kitahara, *J. Stat. Phys.* **9**, 51 (1973).
- ³²K. Kitahara, *Adv. Chem. Phys.* **29**, 85 (1975).
- ³³R. Graham, D. Roekaerts, and T. Tél, *Phys. Rev. A* **31**, 3364 (1985).
- ³⁴B. Peng, K. L. C. Hunt, P. M. Hunt, A. Suárez, and J. Ross, *J. Chem. Phys.* **102**, 4548 (1995).
- ³⁵F. Baras, M. Malek Mansour, and C. Van Den Broeck, *J. Stat. Phys.* **28**, 577 (1982).
- ³⁶F. Baras, J. E. Pearson, and M. Malek Mansour, *J. Chem. Phys.* **93**, 5747 (1990).
- ³⁷F. Baras, in *Stochastic Dynamics*, Lecture Notes in Physics, edited by L. Schimansky-Geier and T. Poeschel (Springer-Verlag, Berlin, 1997), pp. 167–178.
- ³⁸W. Vance and J. Ross, *J. Chem. Phys.* **105**, 479 (1996).
- ³⁹G. Nicolis, *Introduction to Nonlinear Science* (Cambridge University Press, Cambridge, 1995).
- ⁴⁰P. Gaspard, *J. Chem. Phys.* (submitted).
- ⁴¹D. Gonze, J. Halloy, and A. Goldbeter, to appear in *J. Biol. Phys.* **28**, (2002).